Journal of
Nuclear Medicine & Radiation Therapy

Mohymen et al., J Nucl Med Radiat Ther 2014, 6:4
DOI: 10.4172/2155-9619.1000230

Research Open Access

Evaluation of the Impact Count Recovery Model on Standardized Uptake Value Used in PET-CT

Ahmed Abdel Mohymen[1,*], Ahmed Soltan[2] and Hamed Farag[1]

[1]*Radiotherapy and Nuclear Medicine Department, National Cancer Institute, Cairo University, Egypt*

[2]*Biophysics Department, Faculty of Science, Cairo University, Egypt*

Abstract

Evaluate the effect of lesion size and Sphere to Background Ratio (SBR) on the threshold used for PET tumor volume delineation.

Evaluation the effect and the accuracy of Recovery Coefficient (RC) model on Standards Uptake Value (SUV) of different inner size diameters filled with different activity concentration and apply this model on small cohort of patients and construct Look Up Table (LUT) for different lesions with different sizes. A cylindrical phantom equipped with different volume hollow spheres was used. Two different reconstruction algorithms were applied in this study; one of them modified with Point Spread Function (PSF), the other did not based on PSF.

Partial volume effect (PVE) was highly dominant in low uptake spheres although it had large size i.e., not only small size object affecting by PVE but also low activity concentration object. For true volume measurements, practically TrueX algorithm was more accurate when activity measurements deal with true or measured volumes.

Also, the results showed using that phantom study had successfully provided a practical "Look Up Table" for the partial volume correction of spherical lesions at maximum measured activity ratios that were typically noted in human PET-CT imaging. The present study demonstrated that SBR did not have significant effect on the estimation of volumes from PET images in the different SBRs. The only determining factor for the threshold for PET volume estimation was the size of the sphere. Superior percent accuracy was shown for OSEM algorithm when applying RC model to corrected SUV values and OSEM was more efficient and less error variation with respect to sphere volume, but in case of uncorrected data, no remarkable difference between TrueX and OSEM algorithm had been observed.

Keywords: OSEM; PSF; SUV; RC; PVE

Background

The Positron Emission Tomography (PET) is increasingly used for the diagnosis and management of several diseases, with fundamental applications in oncology and radiotherapy (RT). Usually the PET equipment is associated to a Computed Tomography (CT) scanner, to allow an accurate correction of the photon attenuation in patient and an easier anatomical localization of the areas of abnormal uptake of the radiopharmaceuticals. The PET images interpretation in fact is based on the knowledge of the radiopharmaceutical distribution in organs and tissues of patient, and physicians often use quantitative information extracted from images [1], such as the SUV (Standardized Uptake Value) which calculated from:

$$SUV = \frac{\text{activity concentration in tissue}}{(\text{injected activity} / \text{body size})} \quad (1)$$

In order to perform a diagnosis, to compare individual cases with the literature and to extract a Biological Target Volume (BTV) for RT planning. For these reasons, particular importance should be given to image quality and quantitative accuracy of PET/CT scans [1].

SUV is the semi-quantitative method most commonly to determine FDG uptake in attenuated corrected pet images. With this technique, the tumor FDG concentration is normalized to the amount of injected activity and total volume of distribution. Numerous indices have been used to represent the volume [2].

The measured radioactivity within the ROI is normalized to the average radioactivity concentration in the body, which is approximated as the injected dose divided by patient body size [3].

One of the main problems affecting SUV values is partial volume effect which is a complex process affected by many factors including tumor size and shape, background activity in surrounding tissues, spatial resolution of the scanner, image sampling and voxel size, and measurement method. Partial volume effect occurs when radioactive counts from a source or focus "spill out" into a region that is volumetrically larger in the reconstructed image than its physical size. Each PET scanner has an intrinsic point spread function (PSF) which is a profile of how much spread in a reconstructed image occurs when imaging a point source in air. The width of this PSF, which is characterized by measuring the full width at half maximum (FWHM), is usually used as a measure of spatial resolution.

As long as objects of interest are greater than two times the FWHM, the partial volume effects are not very significant. However, if the object is less than two times the FWHM, a significant fraction of the counts "spill out" of the reconstructed object.

***Corresponding author:** Ahmed Abdel Mohymen, Radiotherapy and Nuclear Medicine Department, National Cancer Institute, Cairo University, Egypt, Tel: 00201281549950; E-mail: am_nci@yahoo.com

Received April 20, 2015; **Accepted** May 29, 2015; **Published** June 02, 2015

Citation: Mohymen AA, Soltan A, Farag H (2015) Evaluation of the Impact Count Recovery Model on Standardized Uptake Value Used in PET-CT. J Nucl Med Radiat Ther 5: 230. doi:10.4172/2155-9619.1000230

The spatial resolution in PET images is limited by the detector design (by the pitch of the crystal in the axial direction, for instance) and by the reconstruction process.

Partial Volume Effect (PVE) actually refers to two distinct phenomena, Spillover effect is the first effect and image sample effect (tissue fraction effect) the second effect that make intensity values in images differ from what they ideally should be [4].

PVE depends on the lesion size, the intrinsic contrast between lesion and background, and the aforementioned spatial resolution, which derived from detectors characteristics, reconstruction methods and smoothing filters used. Also the image sampling (i.e. voxelization) produces PVE [1].

One of the methods used to make a correction to PVE at regional level called RC which is the percentage underestimation of the uptake measured in hollow spheres inserted in a cylindrical phantom [4].

Defining the region used to quantify tumor uptake done by several different possibilities and SUV_{max} and SUV_{avg} were concerned.

The TrueX algorithm uses a scanner specific point spread function which is incorporated into the system matrix, resulting in better resolution and noise properties. In this work, the influence of different SBRs, sphere sizes and advanced reconstruction algorithms on target delineation were studied, i.e. the influence of these factors on the threshold and on the activity in the delineated sphere volume was examined in detail. Also we applied Recovery Coefficient (RC) model to make a correction for partial volume effect physically and clinically and show the accuracy of that model after applying and comparing the results yielded of the two algorithms had been used.

Materials and Methods

1. The Jaszczak phantom (Data Spectrum corporation) consists of a cylinderic shaped water-filled cavity with six hollow spherical inserts with inner diameters of 9.9 mm, 12.4 mm, 15.6 mm, 19.7 mm, 24.8 mm, and 31.2 mm suspended by plastic rods. The BG volume of the cavity was 6.9 liters (Figure 1).

2. These spheres were filled with an activity four times of the background (BG), to give different sphere/background ratios (SBRs). These SBRs was calculated from activity concentrations derived from activity measurements in a dose calibrator at filling time. The BG activity concentration was measured at ten ROIs with a diameter matching with each sphere in the peripheral region of the phantom and the mean value of all ROIs was considered as BG activity concentration or calculated by dividing the sphere activity by the BG activity measured in the reconstructed image [5].

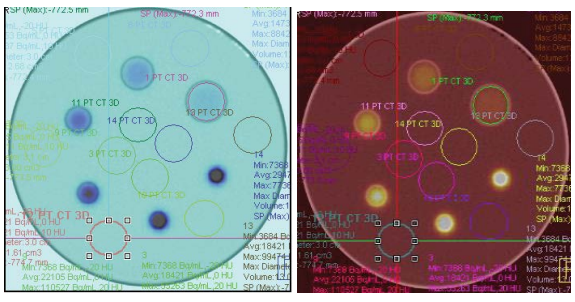

Figure 1: Example of defining ROIs for hot sphere and background activity measurement as set forth by the NEMA convention. Shown is a transverse slice through the phantom, and the green ROI is for the 3 cm hot sphere and the other colors ROIs are for the background.

3. The phantom was filled with an ^{18}F solution of ~1.8 mCi radioactivity and the duration of scanning was 5 min to obtain a statistically reliable number of counts. The Siemens acquisition protocol for whole body PET-CT acquisition with F^{18} was used [6].

4. All measurements were performed on a Siemens Biograph 16 True Point PET/CT scanner (Siemens Medical Solutions), installed at the Department of Nuclear Medicine at the Cancer Children Hospital(CCH).

5. Each measurement was reconstructed with two different reconstruction algorithms available at the Siemens Syngo workstation (Syngo MI workplace, 2008): Iterative Ordered Subsets Expectation Maximization algorithm (3D-OSEM), Iterative TrueX (3D-OSEM+PSF) algorithm.

6. For the two reconstructions algorithm a Gaussian Filter with 5 mm FWHM was applied and a 168 x 168 Matrix was used. For the two iterative reconstruction algorithms, 4 iterations and 8 subsets (i.e., Equivalent Iteration EI=32) were used (clinical standard reconstruction algorithm for FDG PET images recommended by Siemens Medical Solutions).

7. The standards used by NEMA for image quality determination were used to define the ROIs, Rosslyn et al.

8. Evaluation methods

The following quantities were investigated: Threshold and Activity analysis which are described briefly in the following:

Threshold (TH): was determined as a percentage of the maximum activity in a region of interest (ROI).

The threshold is defined by the minimum deviation between measured and true volume and given as the percentage of the source activity concentration [7].

The optimal threshold for defining the true sphere volume was found by manually varying the threshold of the maximum activity and increasing or decreasing the threshold until the true sphere volume was reached. The mean threshold of the large sphere was calculated for different SBRs and fitted using the function:

$$TH = a + b/SBR \quad (2),$$

where a and b are fitting parameters, calculated by linear regression (least square method) of the measured data on the inverse of the SBR.

Activity analysis

In this work the estimated activity is calculated by either the maximum activity concentration or the mean activity concentration measured from the image of the sphere, multiplied by the sphere volume.

The maximum activity of the sphere was defined as the value in the hottest voxel multiplied by the sphere volume. This method was applied, since it is most common in clinical practice. The mean activity in the sphere was calculated by summing up all voxel values in the respective sphere volume.

The Recovery Coefficient (RC) was defined as the "apparent activity concentration in the image divided by the true activity concentration". The calculation of RC was performed by dividing the measured activity

by the true activity in the respective ROI. Since the maximum and the mean activity were investigated, RC_{max} and RC_{mean} were studied.

Since RC represents a measure for the deviation from the true activity, an explicit correction factor C was introduced for clinical convenience such that the multiplication of the measured activity with C results in the true activity. C is simply the inverse of RC and was calculated for all SBRs, sphere sizes and reconstruction algorithms.

As recommended by the manufacturer when using the TrueX algorithm, the mean activity approximates the true activity best. (RC_{mean} used instead of RC_{max}) for TrueX.

The correction factor C, which was introduced to reproduce the true activity, can be calculated for every single reconstruction algorithm using:

$C_{algorithm}$=A ∗ exp (B/sphere volume), (3)

With the fitting parameters **A** and **B** [ml], derived from the calculated data [**8**]

"Attenuation correction for phantom was performed by CT transmission scan "

9. The relationships between optimal threshold (%) and the estimated SBRs for the two reconstruction techniques were plotted.

10. The relationships between (RCmax & RCmean) and different sphere volumes for the two reconstruction algorithms were plotted.

11. The relationship between RC versus the measured maximal activity ratios was plotted.

(*Max pixel in hot sphere/average background pixel=maximal activity ratios)* (4) [9]

The relationships between correction factor C_{max} and C_{mean} and different sphere volumes for the two reconstruction techniques were plotted [8].

12. Relationship between the true volume and calculated volume of the spheres was plotted [10].

Patient Studies

Analyzed whole body by ^{18}F-FDG PET-CT studies of small cohort of patient imaging was done for primary staging or treatment evaluation. We worked with different types of malignancies. Patients were injected intravenously with 370–555 MBq (about 10–15 mCi) ^{18}F-FDG, depending on body weight and habits. Images were acquired 45-60 min after infusion. Patients fasted for at least 6 HRs before tracer injection, although liberal water intake was encouraged.

SUV calculations

Coronal images reconstructed with either 3D-OSEM or TrueX were displayed simultaneously on the monitor.

A tumor lesion was defined as abnormal focal ^{18}F-FDG uptake above background level and outside of normal anatomic structures. The SUV was calculated as follows:

$$SUV = \frac{Decay\ corrected\ activity\ (kBq)/Tissue\ volume\ (mL)}{Injected\ activity\ (kBq)/Body\ weight\ (g)} \quad (5)$$

An evaluate to the effect of Count Recovery (RC) model on SUV values of different inner size diameters filled with different activity concentration. Apply the model on small cohort of patients and determine Look Up Table for different lesion with different sizes.

In order to accurately quantify the magnitude of the partial volume effect, a measure of the activity concentration within each sphere and the background was compared to that of the known activity ratio between the spheres and background this was readily achieved with a recovery coefficient (RC). The RC formula is given by the following simple expression:

1. $$RC = \frac{Measured\ spher\ activity - measured\ BG\ activity}{Known\ sphere\ activity - knwon\ BG\ activity} \quad (6)$$

2. This parameter is only justified in the case where the background is not itself subject to Partial Volume Effects, and is of known and uniform activity concentration.

3. The simple formula obtained in Eq. 7 yields the partial volume corrected SUV_{max}.

4. $$PV\ corrected\ activity = \frac{Measured\ activity - BG\ activity}{RC} + BG\ activity \quad (7)$$

5. The effect of incorporation of Point Spread Function into system matrix of TrueX reconstruction algorithm obtained by comparing the partial volume corrected SUV_{max} yielded from 3D-OSEM and that yielded from TrueX.

6. To give some practical idea of how partial volume correction could be carried out in a clinical population, we applied this correction method to a limited number of patients. The maximal diameter of the lesion was obtained from the PET-CT patients images which may have been with or without iodinated contrast and the maximal activity ratio was obtained by placing a ROI around each lesion to obtain the SUV_{max} and the surrounding territory to obtain the background SUV_{mean}.

7. Dividing the lesion SUV_{max} and the background SUV_{mean} gives the maximal activity ratio. Using these parameters, the appropriate RC was determined from the "Look Up Table" [9].

8. At this point, all the values for the correction were available, and inserting them into the simple formula obtained in Eq. 7 yields the partial volume corrected SUV_{max}.

Results and Discussion

Evaluation methods

The calculations of the fitting functions required for the threshold and activity analysis were done by using Microsoft Office Excel 2007.

Threshold: The relationship between the best threshold of activity to accurately measure the true volume of the spheres and the measured SBR ratio were determined for the two reconstruction algorithms as shown in Figure 2.

These relationships presented in Figure 2 indicated that for high contrasted objects (low SBR ratio; a lower threshold of activity had to be applied to adequately measure the actual volume of the spheres. Also, for a given SBRs ratios, the threshold to be applied depended on the reconstruction algorithm but Daisne et al. [11] proposed that for less contrasted objects (low SBR ratio), a higher threshold of activity had to be applied to adequately measure the actual volume of the spheres.

The present work indicated that the threshold values are increasing with decreasing sphere sizes for all spheres and the increasing in smaller spheres is higher for TrueX than OSEM, Also, it is observed that the largest sphere containing low activity concentration, high contrast, low threshold, and low SBR and vise versa for the smallest sphere.

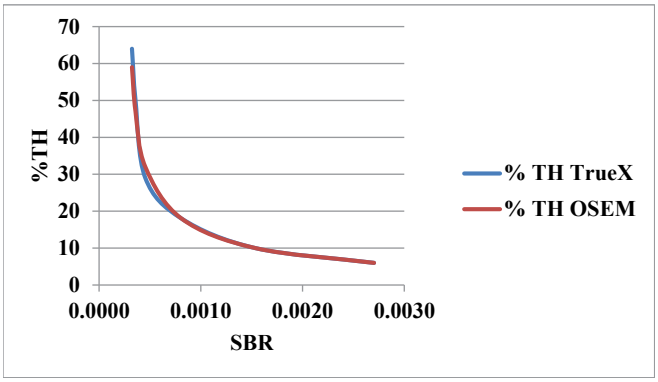

Figure 2: Threshold defining the true sphere volume as function of the SBR using the OSEM and the TrueX algorithm, the data were fitted through an inverse function which provided the best regression parameters.

Our data referred that the threshold values decreased with increasing sphere size because it containing low activity concentration but [5] stated that the threshold values for PET based target volume segmentation increased with increasing sphere size for the two algorithms, which can be regarded as constant for larger spheres volumes and dependent on the SBR.

Threshold varied according to the signal to background (SBR) ratios, being typically higher for less contrasted images which agree with our previous published work [12].

For small structures, the partial volume effect becomes more pronounced and a significantly reduced apparent activity concentration was observed but in our work partial volume effect is highly dominant in low uptake spheres although its large size i.e., not only small size object affecting by PVE but also low activity concentration object.

The diameter and volume of each sphere was successively calculated using increasing thresholds, where the thresholds were determined as a percentage of the maximal activity in the spheres. The optimal thresholds which resulted in minimal least square difference between measured and actual sphere volumes were obtained.

The volumes of the spheres were calculated by applying a threshold of activity as a function of the measured signal to background ratios.

The relationship between threshold percentage of the two reconstruction algorithms and the true volumes of different spheres which containing different activity concentrations yielding SBR threshold volume curve shown in Figure 3.

In Figure 3 simple parameterization of the calibration curves for the two reconstruction algorithms using the following function

$$TH(V) = m/V + TH \quad (8)$$

(TH=the upper threshold, and V=the true volume of the sphere) [13].

The relationship between %TH versus 1/V shown in Figure 4 yielding a straight line with the slope m and the intercept TH.

The slope and intercept were determined using a linear regression technique of the measured data on the inverse of the sphere volume.

In the present work, different activity concentrations in different spheres which leading to different SBR so, threshold increase with decreasing sphere volumes this means the threshold values calculation of affecting by activity concentration but [13] considered that according to the selected SBR threshold volume curve, there is a fixed threshold value T1 (fixed threshold region) for large volumes.

The adequate estimate of the volume was observed for spheres between 0.5 and 16.0 ml as shown in Figure 5. The volumes of the spheres were calculated by applying a threshold of activity as a function of the measured signal to background ratios Figure 2. Two different reconstruction algorithms have been used TrueX and OSEM.

Figures 4, 6 and 7 show the relation between percent threshold and inverse of the true and measured volume for both algorithms (Table 1).

For true volume the values of parameters A and B of TrueX algorithm deviate from that of OSEM algorithm by about ±13% and ±10%, respectively.

For measured volume the values of parameters A and B of TrueX algorithm deviate from that of OSEM algorithm by about ±12.7% and ±7.8%, respectively.

The relation between percent threshold of the two reconstruction algorithm and both true and measured volume shown in Figures 3, 8 and 9 for both algorithms. There was a trend for a more accurate estimate

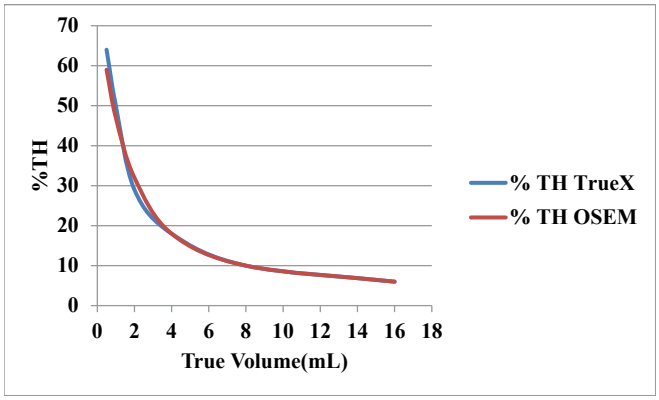

Figure 3: SBR threshold-volume curve determined with NEMA phantom at different spheres sizes with different activity concentrations.

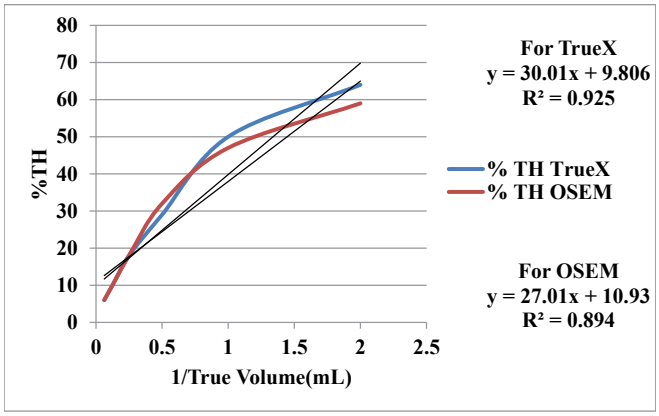

Figure 4: Threshold versus inverse of true volume using the OSEM and the TrueX algorithm.

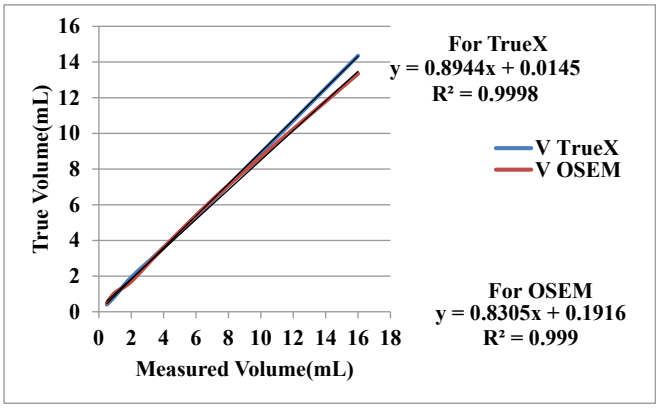

Figure 5: Relationship between the true volume and the measured volume of spheres

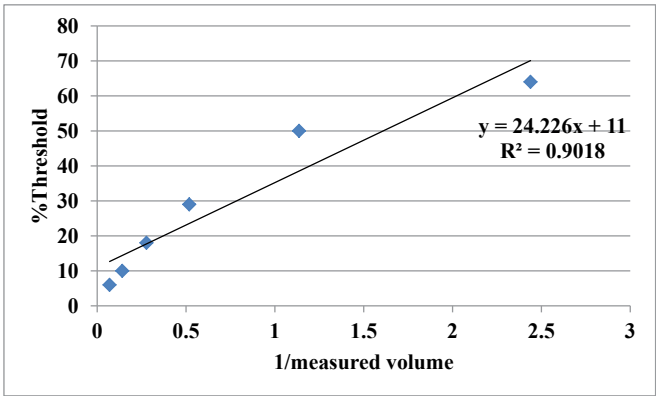

Figure 6: Threshold versus inverse of measured volume using TrueX algorithm.

within the whole range of sphere's sizes using images reconstructed with TrueX and OSEM.

Overall, using the method described in this work, adequate estimate was observed for objects having at least a diameter between once and twice the FWHM. For objects smaller than the FWHM, as the determination of the volume is likely to be influenced by the partial volume effect, the method reported in the present work does not hold anymore.

We observed that partial volume effect dominant in large sphere size due to low activity concentration i.e., not only sphere size leading to arise of PVE phenomenon but also activity concentration.

In small size sphere the over increasing in activity concentration leading to increasing in volume assessment than volume that ideally should be.

Not only does activity from inside the sphere spill out but also activity from outside the sphere spills into the sphere, partially compensating for the spilling out. Obviously, the spilling out (signal from inside the sphere that goes outside the sphere) depends on the uptake inside the sphere. Most often, it is not balanced by the spilling in (signal from outside the sphere that comes inside the sphere); therefore, it is difficult to predict the overall effect of PVE [4].

Using the TrueX algorithm for image reconstruction, the threshold

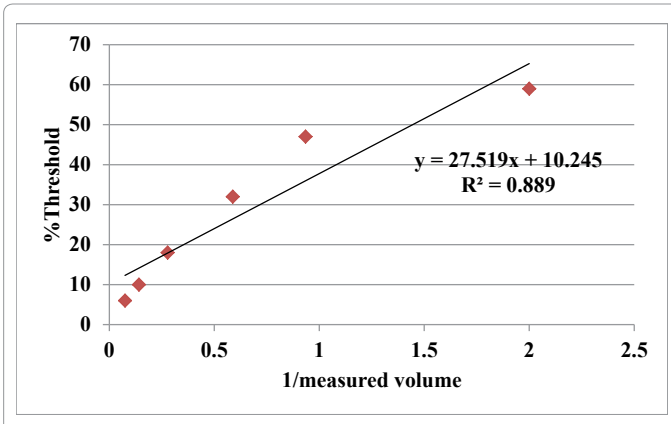

Figure 7: Threshold versus inverse of measured volume using the OSEM algorithm.

	A(ml)	B(mL)	R²
For true volume TrueX	30.52	9.8	0.925
For true volume OSEM	27	10.9	0.894
For measured volume TrueX	24	11	0. 901
For measured volume OSEM	27.5	10.2	0.889

Table 1: The values of A and B (mL) that verify the relation between percent threshold and inverse of the true and measured volume for both algorithms. The data have been fitted through a linear regression.

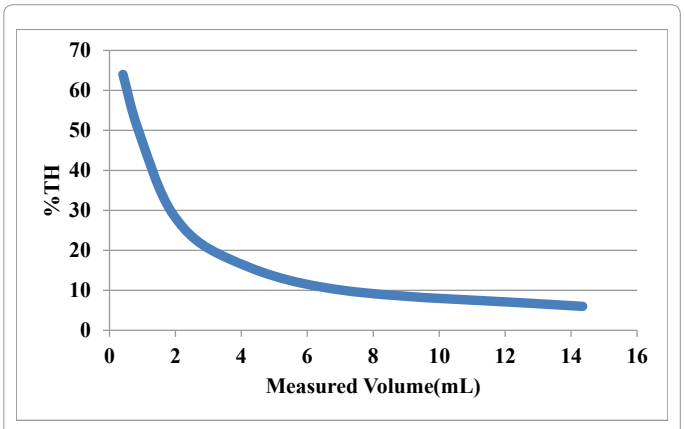

Figure 8: Threshold versus measured sphere volume using TrueX reconstruction algorithm.

defining the true sphere volume was higher comparing to the OSEM algorithm (depending on the SBRs).

The threshold and SBR decreased with increased of sphere size since the smallest sphere contained the highest activity concentration.

Volume underestimation analysis

For each sphere or simulated tumor, the percent bias (%underestimation) in estimated volume was calculated by: [10]

$$\%underestimate\,(\%Evolume) = \left(\frac{measured\ volume}{true\ volume} - 1\right) \times 100\% \quad (9)$$

Note that; bias may be negative, indicating underestimation of the sphere volume and vice versa for positive bias.

To verify the validity of the relationships established above, the volumes of the spheres were calculated by applying the threshold of activity determined as a function of the measured SBR ratios. Typically, for the two reconstruction algorithms, the volumes of the different spheres sizes were differed in estimation and the percent error in volume estimation was higher for smaller spheres than larger spheres as shown in Table 2. This can be attributed to the difference in activity concentration among the six spheres; the smallest sphere volume has the highest activity concentration and the largest sphere volume has the lowest activity concentration.

The %E volume underestimation was observed for the four largest spheres 16 ml, 8 ml, 4 ml, 2 ml.

In the largest sphere volume the %E volume underestimation for both TrueX and OSEM were -16.3% and -22.6% respectively.

The %E volume underestimation for 8 ml, 4 ml was the same -11.3% and -1% respectively for both algorithms.

For 2 ml sphere volume the %E volume underestimation was higher for TrueX than OSEM.

For 1 ml sphere volume the %E volume overestimated for both algorithms but obtain similar values.

Dramatically higher variation in %E volume was observed for both algorithm in the smallest sphere volume 0.5 ml and the %E volume was overestimated by 22% for TrueX and underestimated by -18% for OSEM.

In spite that, Figure 10 represents the real deviations in imaging determining the sphere volume comparing to the real sphere volume, really it is found that these deviation did not match physically. It is noticed that heterogeneity in these deviations, it can be referred as a background difference effects and it is not volume sphere dependence.

According to the previous values TrueX algorithm may lead to an overestimation of the true activity for measurements with active background which is confirmed by ref. [5].

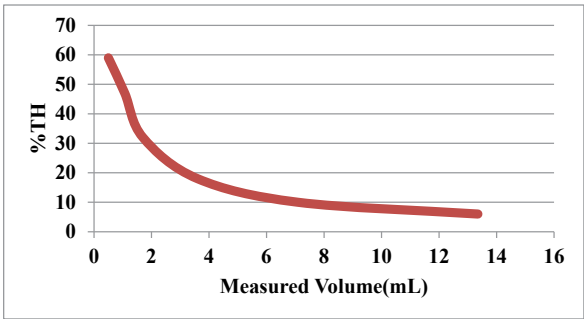

Figure 9: Threshold versus measured sphere volume using the OSEM reconstruction algorithm.

V_{true} mL	$V_{measured}$ TrueX	$V_{measured}$ OSEM	$\%E_{volume}$ (TrueX)	$\%E_{volume}$ OSEM
16	13.39	12.39	-16.3125	-22.5625
8	7.09	7.09	-11.375	-11.375
4	3.96	3.96	-1	-1
2	1.6	1.7	-20	-15
1	1.06	1.06	6	6
0.5	0.61	0.41	22	-18

Table 2: The accuracy of the threshold method in estimating the spheres volume using two different reconstruction algorithms TrueX and OSEM.

The use of FDG-PET for the delineation of the tumor volume is becoming increasingly popular in oncology for the estimation of metabolic tumor burden and for radiotherapy planning. Although many methods have been proposed for tumor volume delineation in F ^{18}FDG PET images, there is no consensus regarding which method should be preferred [14].

Differences in imaging parameters can have a pronounced effect on the performance of semi-automated methods to delineate tumors. This implies that PET data collection and image reconstruction procedures and the semi-automated tumor delineation methods need to be standardized and calibrated for each scanner for reproducible and accurate tumor delineations [15,16].

Herzog et al. [17] pointed out that although tomographic imaging has substantially benefited from the introduction of statistical image reconstruction, advanced iterative reconstruction algorithms have to be used carefully.

Activity analysis: The correction factor C, which was introduced to estimate the true activity, can be calculated for both reconstruction algorithms using equation (3).

The relationship between the measured volumes using the two reconstruction algorithms obtained when applying the threshold and the correction factor C represented in Figures 11 and 12 for both algorithms. These were lead to the values of C_{TrueX} and C_{OSEM} and when comparing this values with that obtained from the relation between the correction factor C and true volume Figure 13. We can conclude that the values of C_{TrueX} and C_{OSEM} is nearly the same for both measured and true volumes relationships.

The correction factor (C_{mean}) parameters (A&B) for the two reconstruction algorithms obtained when plotting the relation between $C_{algorithm}$ and inverse of the true volumes shown in Table 3.

Table 3 show the values of A and B [mL] that verify the relationship between the $C_{algorithm}$ and the inverse of the measured and true volumes obtained from Figures 14-16 respectively. We can define that the values of A and B is nearly equal and the residual error is nearly the same.

Figure 16 represents $C_{algorithm}$ versus the inverse of true sphere volume using the OSEM and the TrueX algorithm.

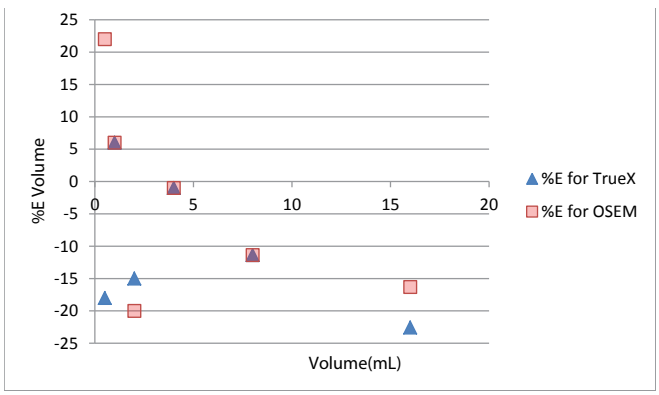

Figure 10: Fractional deviations of the automatically determined sphere volumes compared to the true values.

For true volumes Figure 13: the values of $C_{algorithm}$ could be detected as C_{TrueX} =2.8 and C_{OSEM}=2.9.

For measured volumes Figures 11 and 12: the values of $C_{algorithm}$ could be detected as C_{TrueX}=2.9 and C_{OSEM}=3.

$C_{algorithm}$ decreased by increasing measured volume for both TrueX and OSEM as shown in Figures 11 and 12.

For measured volume we obtained that the values of parameters A and B of TrueX algorithm deviate from that of OSEM algorithm by about ±16.8% and ±7.7% respectively.

For true volume we obtained that the values of parameters A and B of TrueX algorithm deviate from that of OSEM algorithm by about ±22% and ±7% respectively.

We can conclude that for true volume measurements TrueX algorithm practically is more accurate when activity measurements deal with true or measured volumes.

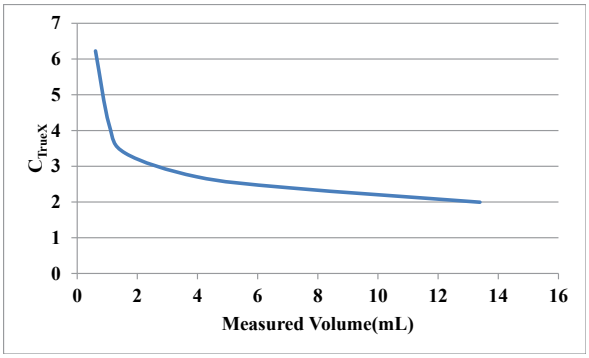

Figure 11: measured volume versus correction factor for TrueX algorithm.

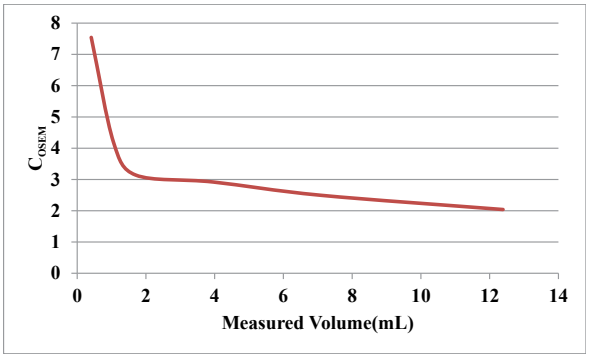

Figure 12: Measured volume versus correction factor for OSEM algorithm.

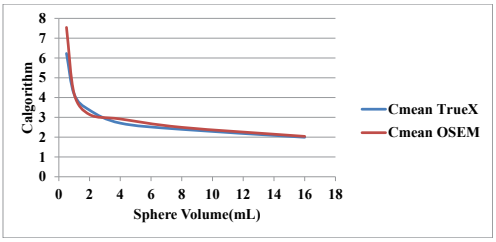

Figure 13: Correction factor C for receiving the true activity: C_{OSEM} for the mean activity and C_{TrueX} for the mean activity.

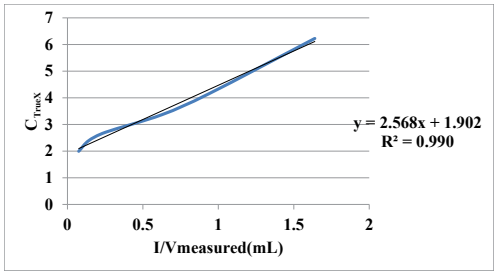

Figure 14: $C_{algorithm}$ versus inverse of measured sphere volume using the TrueX reconstruction algorithm.

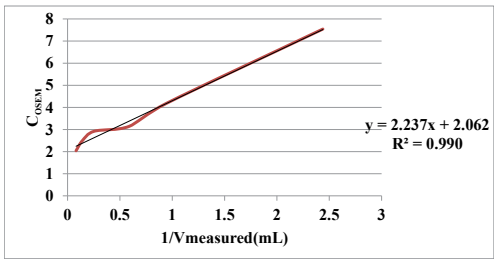

Figure 15: $C_{algorithm}$ versus inverse of measured sphere volume using the OSEM reconstruction algorithm.

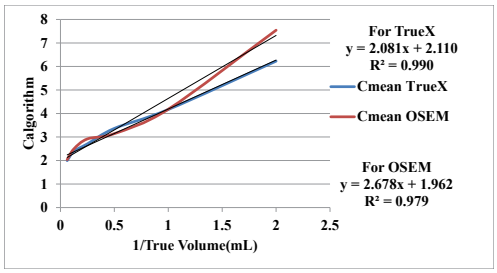

Figure 16: $C_{algorithm}$ versus inverse of true sphere volume using the OSEM and the TrueX reconstruction algorithms.

Since, there is no significant difference between the maximum activities for both algorithms, we considered that C for both algorithms refers to the mean activity and our data confirm that recovery coefficient depend on the lesion size, the sphere to background ratio (SBR).

The values of C ($C_{algorithm}$=1/RC_{mean}) is nearly constant for the large spheres 16 mL, 8 mL, 4 mL but highly increasing for small spheres 2 mL, 1 mL, 0.5 mL as shown in Figure 13. It is clearing from these curves that RCs are highly dependent on the size of the lesion which is completely agree with the findings obtained by Knäusl et al. [5], these findings states that for the largest three volumes a constant factor C was found. For smaller volumes, C increased exponentially due to the partial volume effect.

The data presented in Figures 17 and 18 confirm that RC is inversely proportional to activity concentration which means that as SBR increase, the RC decrease.

Knäusl et al. [5] indicated that the threshold values for PET based target volume segmentation increased with increasing sphere size for

both algorithms, which can be regarded as constant for sphere volumes larger than 2.5 ml and are dependent on the SBR but in our works threshold values increase with decrease sphere sizes due to differences in SBRs. Experimentally determined correction factors C were obtained in order to be able to calculate the true activity. Even though the TrueX algorithm with Gaussian filter produced artificial results for small spheres, for large spheres the maximum activity represented the true activity well also without correction, as it is the case for the OSEM algorithm. But, according to the manufacturer's recommendation the mean activity should be used in combination with the TrueX algorithm. However, if the mean activity is applied in studies, an appropriate correction is essential for quantitative assessment of the PET result. When using the TrueX algorithm for quantitative evaluation, especially in follow up and multicenter studies, commonly accepted guidelines concerning the staging have to be used with care.

Partial volume correction using Recovery Coefficient (RC) model

In order to accurately quantify the magnitude of the partial volume effect, a measure of the activity concentration within each sphere and the background was compared to that of the known activity ratio between the spheres and background. This was readily achieved with a recovery coefficient (RC).

Figures 17a and 17b demonstrates the characteristic logarithmic curves that are generated when the relationship between RCs of the two reconstruction algorithms versus diameters (cm) of the spheres. RCs decreased for the two reconstruction algorithm as the diameters (cm) decrease in spheres 3 to 1 cm which is agree with Srinivas et al. [9].

When the relationship between the RCs values of the two reconstruction algorithms versus the measured maximal activity ratios derived from the two algorithms (max pixel in hot sphere: average background pixel) were plotted and presented in Figures 18a and 18b) for TrueX and OSEM respectively. It is noticed that the measured maximal activity ratio is always less than the true activity ratio due to the partial volume effect and MAR increasing with decrease sphere sizes which disagree with Srinivas et al. [9], since in our works the activity concentration is highest in the smallest sphere but lowest in the largest one.

From equation (6) RCs values obtained and knowing the measured activity of the spheres and background activity hence, all the values for the correction were available, and when using them into the simple formula obtained in equation (7) that yields the partial volume corrected SUV_{max} as shown in Table 4.

We noticed that after applying the RC model the losses in the measured data were compensated and slightly differences between

	A(ml)	B(ml)	R^2
For true volume TrueX	2.08	2.1	0.99
For true volume OSEM	2.68	1.96	0.979
For measured volume TrueX	2.57	1.9	0. 99
For measured volume OSEM	2.2	2.06	0.99

Table 3: Parameters of the correction factor C_{mean} for the two reconstruction algorithms resulted when plotting the relation between $C_{algorithm}$ and inverse of the true and measured volumes. The data have been fitted using a linear regression.

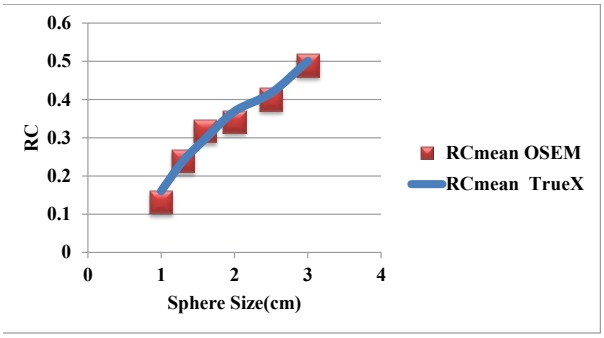

Figure 17a: Sphere diameter versus RC_{mean} using the OSEM and the TrueX algorithm.

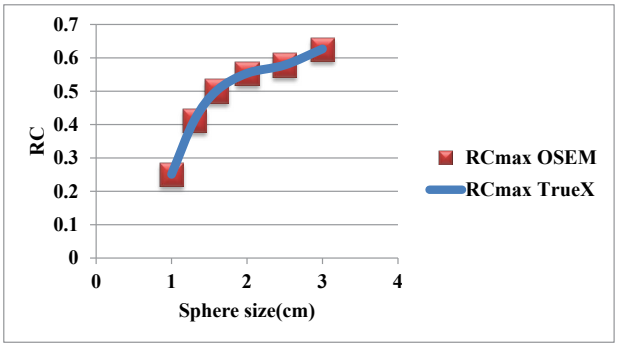

Figure 17b: Sphere diameter versus RC_{max} using the OSEM and the TrueX algorithm.

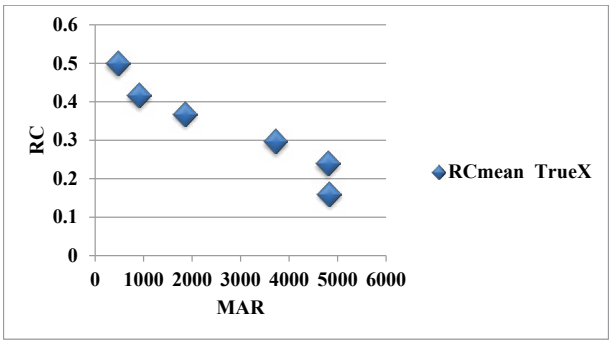

Figure 18a: RC versus (MAR) for TrueX algorithm.

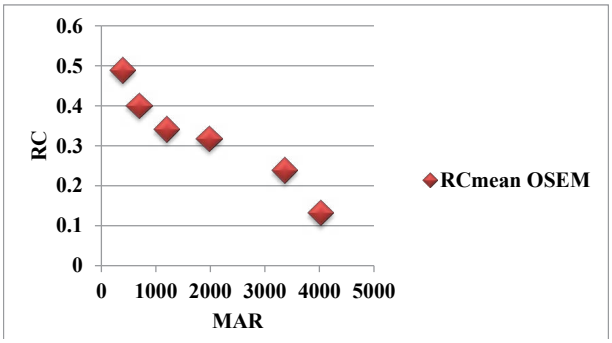

Figure 18b: RC versus (MAR) for OSEM algorithm. algorithm.

the true activities concentration of the spheres at filling time and the corrected measured activities concentration were shown in Table 4 as PVcorr SUV.

The threshold for large spheres was independent of sphere size, since the sphere diameter was large compared to the spatial resolution, however the threshold depended on the SBR.

The SBR threshold volume curve Figure 2 appears to be slightly dependent on the type of image reconstruction algorithm especially for small structures and on the spatial resolution of the imaging device.

For smaller spheres with higher SBR which contain the maximum activity concentration it is noticed that the smaller the sphere diameter, the higher the SBR underestimation.

The optimum threshold values were consistently higher for the TrueX images because the source activity concentration is in general underestimated compared with the values for the OSEM reconstructed images.

Because of signal loss and limited spatial resolution, an underestimation of the maximum activity for all sphere volumes was expected. This underestimation should be in the range of a few percent for large sphere sizes and increase substantially with decreasing sphere volume. In addition, the spatial resolution had a partial effect on spheres detection since the activity concentration was lower in large sphere and higher in small sphere so the underestimation was higher for smallest spheres in contrast to largest one.

In images reconstructed with OSEM algorithm, RC_{max} was found to be independent of the SBR for all spheres. RC_{max} showed a systematic correlation to the sphere size and could be fitted using a logarithmic function.

RC_{mean} was lower for all sphere volumes and decreased with decreasing sphere sizes. In general RC_{mean} showed the same systematic behavior like RC_{max}.

As recommended by the manufacturer when using the TrueX algorithm, the mean activity approximates the true activity best. Figures 17a and 17b shows the RC_{mean} and RC_{max} as a function of spheres sizes for different activity concentration spheres, RC_{mean} showed the same systematic behavior like in OSEM reconstructed images.

It is clear from these Figures 17a and 17b that RCs are strongly dependent on the size of the spheres. Also RCs values were slightly higher for TrueX than OSEM this indicated that TrueX algorithm is higher in activity determination than OSEM.

The main of this work aimed to generate a "Look Up Table" to determine approximate RC values for lesions of different sizes when partial volume correction was desired. Using Figures 17 and 18 as such, two pieces of key information are needed: one is the measured maximum activity ratio and the second is the physical size of the object. The first can be obtained using ROI analysis from the PET scan, and the second obtained easily from CT images. Of course, the assumption is that the structural imaging technique will provide a reasonably accurate estimate of the true size of the object of interest on the PET images.

With regard to using "Look Up Table" to improve diagnosis in solitary pulmonary nodules, it is clear that the net effect of partial volume correction is to modify the SUV. Small lesions with SUVs ***2.5*** will very likely become greater than 2.5 (and lesions greater than 2.5 will become even higher).

The most important application of this RC technique for partial volume correction is likely to be in further studies when measuring the absolute true activity of a lesion is desirable for the designed experiment. In such settings, this approach may be beneficial for generating optimal results.

Accuracy of PVC method

PVC was applied to the pixel value estimates and the percent biases (%E) of the estimated mean pixel values relative to the true values were calculated based on following equation:

$$\%E = \left(\frac{PVC\ SUV}{SUV} - 1\right) \times 100\% \quad (10)$$

Note: negative values of the bias indicate underestimates of the activity in a ROI should be taken into consideration.

Generally it is observed from Table 5 that OSEM is more efficient for introducing corrected data than TrueX that is due to the physical parameters (Recovery Coefficient model) dealing with OSEM can determine the activity concentration in a good precision than the parameters of TrueX, i.e., RC model gives better accuracy when applied to OSEM than TrueX.

Recovery correction (Figures 19a and 19b) show the fractional deviation of uncorrected and corrected SUV_{mean} from the known true activity value for RC method.

Superior percent accuracy is shown for OSEM algorithm when applying RC model to corrected SUV values and OSEM is more efficient and less error variation with respect to sphere volume as shown in Figure 19a, but in case of uncorrected data we did not observe a remarkable difference between TrueX and OSEM algorithm as shown in Figure 19b.

As expected, the uncorrected data clearly exhibit a reduced mean recovery. The reduction is size dependent and affects even the largest investigated target structures which agree with the work. For both algorithms before correction it is noticed that the underestimation is

True activity conc.(kBq/ml) at filling time	Max TrueX before correction	Mean TrueX before correction	Max OSEM before correction	Mean OSEM before correction	Pvcorr SUVmax for TrueX	Pvcorr SUVmean for TrueX	PVcorr SUVmax for OSEM	PVcorr SUVmean for OSEM
15493	9800	7770	9800	7600	15632	15519	15684	15528
29600	17212	12364	17212	11866	29746	29626	29746	29642
60125	33367	22201	33367	20598	60264	60151	60235	60183
118400	59494	35180	59349	37671	118465	118426	118509	118469
244200	100722	58560	100722	58409	244277	244254	244328	244291
481000	120720	77247	120720	63762	481075	481105	481171	481165

Table 4: The true activity concentration (kBq/ml) and maximum and mean measured activity concentration for both algorithms and PVcorr $SUV_{max,mean}$ for both algorithm that obtained when applying recovery coefficient model.

gradually increased as the sphere size increased Figure 19b. On the other side, for TrueX algorithm after correction it is noticed that the overestimation is nearly the same for 0.5,1 and 2 mL sphere volume, but started to increase in steps as the sphere volume increased as shown in Table 5 and Figure 19a but for OSEM the overestimation increase in steps as the sphere volume increased. This can be attributed completely to the remarkable differences in activity concentration between the smallest sphere and the largest one.

One limitation of this phantom study is that it cannot be directly implemented in other institutions. Although a similar relationship between the signal to background ratio and the isoactivity level is expected, the data must be reprocessed each time a new reconstruction algorithm and/or a new camera are used to adjust the parameters 'a' and 'b' of the inverse relationship described. Another limitation is that it did not address the issue of objects with complex shape usually observed in clinical situations.

Sp.vol / %E	%E for TrueX (Corr.)	%E for OSEM (Corr.)	%E for TrueX (Uncorr.)	%E for OSEM (Uncorr.)
16	0.167	0.224	-0.49851	-0.50948
8	0.089	0.143	-0.5823	-0.59912
4	0.045	0.097	-0.63075	-0.65741
2	0.023	0.058	-0.70287	-0.68183
1	0.022	0.038	-0.7602	-0.76081
0.5	0.022	0.034	-0.8394	-0.86744

Table 5: the accuracy before correction and after applying recovery coefficient model to make a correction for the effect of partial volume.

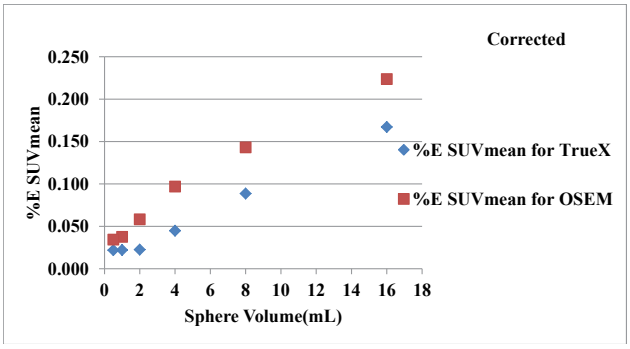

Figure 19a: Accuracy of delineation method as a function of sphere sizes. The corrected SUV_{mean} is shown.

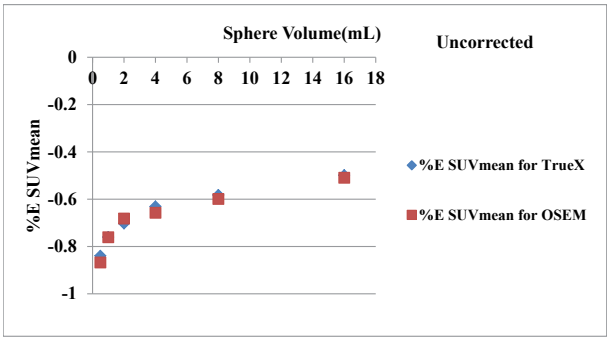

Figure 19b: Accuracy of delineation method as a function of sphere sizes. The Uncorrected SUV mean is shown.

Patient Studies

A tumor lesion was defined as abnormal focal ^{18}F-FDG uptake above background level and outside of normal anatomic structures. The SUV was calculated by equation (5).

SUV_{max} and SUV_{avg} (maximal and average SUV in the ROI) were calculated for each ROI as shown in Figures 20 and 21.

Construction of Look Up Table (LUT) yielded from applying Recovery Coefficient model.

[22]TrueX Look Up Table (LUT): Table 6a Parameters used for calculation of a partial volume corrected SUV_{max} for 22 lesions from 10 patients with different types of malignancies and the patient images reconstructed by TrueX algorithms.

For TrueX algorithm before the correction, all the lesions combined gave an average SUV_{max} of 10.0 and an average lesion size of 2.2 cm. After partial volume correction of each lesion, the average SUV_{max} increased to 16.6 for all the lesions.

OSEM Look Up Table (LUT): In Table 6b parameters used for calculation of a partial volume corrected SUV_{max} for 19 lesions from 10 patients with different types of malignancies and the patient images reconstructed by OSEM algorithms.

For OSEM algorithm before the correction, all the lesions combined gave an average SUV_{max} of 8.7 and an average lesion size of 2.2 cm. After partial volume correction of each lesion, the average SUV_{max} increased to 12.4 for all the lesions.

It is noticed from Tables 6a and 6b that the values of SUV_{max} before applying RC model were ranged between 4.6 and 22.5 and the values after applying RC model were 7.4 and 38.3 for TrueX. For OSEM the same behaviour was noticed.

According to these findings it was easy to say that RC methods may be suitable for the quantification of tumor uptake but not for visual analysis.

A necessary assumption is that the volume and shape of the metabolically active part of the tumor are approximately known. For a spheric tumor, the RC can be readily calculated as a function of the sphere size and the sphere to background contrast for a wide range of spatial resolution values and then used for correction.

The RC depends not only on tumor volume but also on image sampling. The RC can be calculated by assuming no surrounding activity, and the uptake surrounding the tumor, which has to be estimated to compensate for spilling in, can be accounted for subsequently by use of a simple formula when the RC is applied.

The method assumes that the uptake is uniform throughout the tumor although a necrotic part could be excluded if the tumor is delineated and the method usually accounts only for uniform known surrounding activity. If the tumor is close to 2 structures with different uptake values, then the use of the RC may be inappropriate. The correlation between ^{18}F-FDG uptake assessed by SUV_{max} and sphere size observed in non small cell lung cancer (NSCLC) tumors disappeared after PVE correction. This effect occurred because this relationship was attributable mostly to the tissue density, which makes apparent activity depend on tumor size. More puzzling, the correlation between primary NSCLC tumor stage and ^{18}F-FDG uptake measured with SUV_{max} also disappeared after PVE correction. This result could suggest

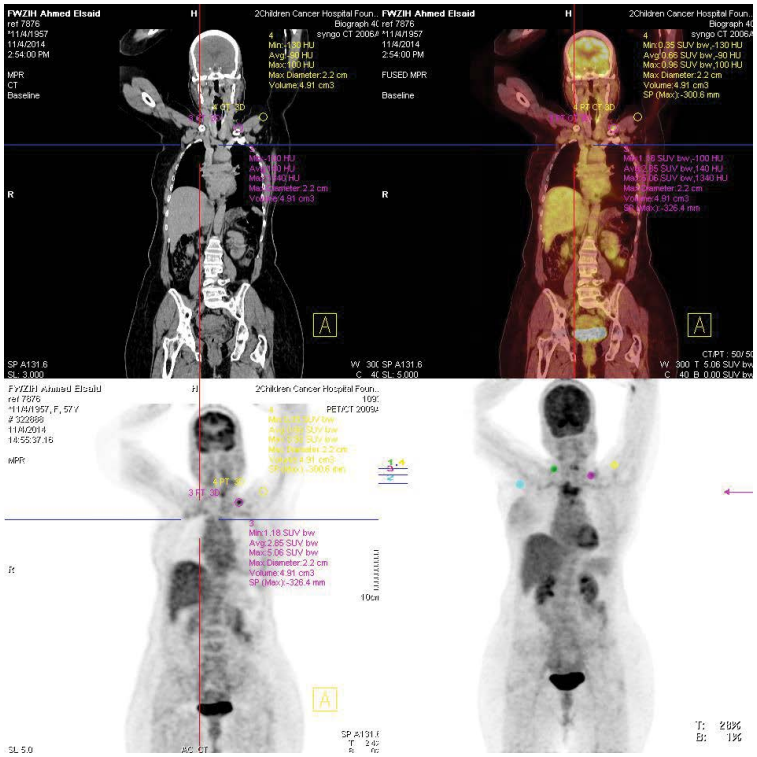

Figure 20: Patient example: Coronal PET images of 58-y-old male with diffuse lymphoma in neck. ROIs are placed in tumor. SUV max and SUV_{avg} are calculated as shown.

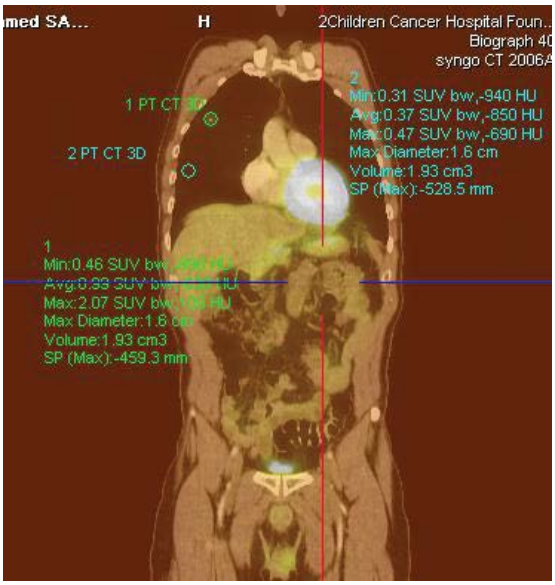

Figure 21a: Patient example 1: Coronal PET images of 53-y-old male with NSCLC. ROIs are placed in tumor. SUV max and SUV_{avg} are calculated as shown.

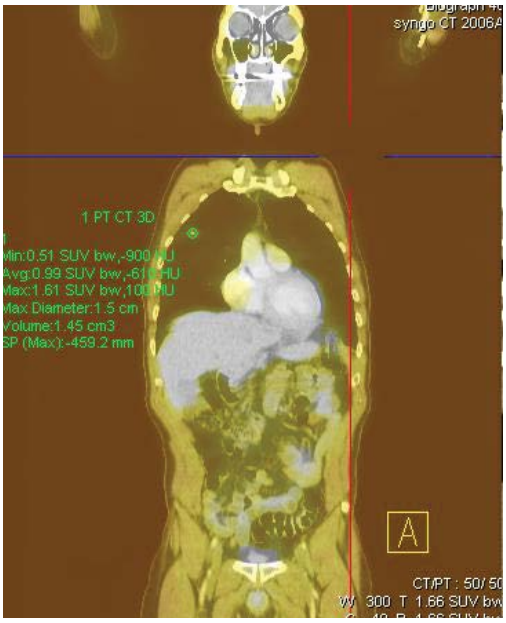

Figure 21b: Patient example2: Coronal PET images of 53-y-old male with NSCLC. ROIs are placed in tumor. SUV max and SUV_{avg} are calculated as shown.

NO.	lesion max (kBq/ml)	bkg mean (kBq/ml)	lesion dia. (cm)	lesion: bkg ratio	RC	Pvcorr (kBq/mL)	SUV (g/ml) AFTER	SUV (g/ml) BEFOR	AFTER/BEFOR
1	31.86	4.70	2.7	6.8	0.587520	50.9	9.4	5.9	1.60
2	35.80	5.07	1.8	7.1	0.587450	57.4	7.4	4.59	1.60
3	70.20	2.18	2.6	32.1	0.582750	118.9	15.2	9	1.69
4	42.12	6.63	2.2	6.4	0.582580	67.5	8.7	5.4	1.60
5	99.36	2.30	1.7	43.1	0.587700	167.4	34.9	20.7	1.69
6	108.00	2.74	2.7	39.5	0.581330	183.8	38.3	22.5	1.70
7	75.84	3.70	2.2	20.5	0.585400	126.9	26.4	15.8	1.67
8	78.67	3.70	2.2	21.3	0.584710	131.9	27.5	16.39	1.68
9	46.08	8.34	3	5.5	0.587750	72.6	12.1	7.68	1.57
10	45.60	22.20	2.7	2.1	0.588400	62.0	10.3	7.6	1.36
11	59.77	4.09	2	14.6	0.586070	99.1	23.0	13.9	1.66
12	35.00	6.45	1.8	5.4	0.587770	55.0	12.8	8.14	1.57
13	76.54	3.18	3	24.1	0.584200	128.8	29.9	17.8	1.68
14	30.68	2.48	1.6	12.4	0.586450	50.6	8.6	5.2	1.65
15	68.44	2.54	1.8	27.0	0.573700	117.4	19.9	11.6	1.72
16	26.31	3.43	2.2	7.7	0.586010	42.5	8.2	5.06	1.61
17	32.60	4.32	2	7.6	0.587010	52.5	10.1	6.27	1.61
18	69.30	7.59	2.3	9.1	0.587010	112.7	17.1	10.5	1.63
19	34.78	5.81	2.2	6.0	0.587680	55.1	8.4	5.27	1.58
20	55.24	4.05	1.9	13.6	0.586260	91.4	12.9	7.78	1.65
21	47.93	6.46	1.8	7.4	0.584000	77.5	10.9	6.75	1.62
22	55.59	5.33	1.8	10.4	0.586825	91.0	12.8	7.83	1.64

Table 6a: Parameters used for calculation of a partial volume corrected SUV_{max} for 22 lesions from 10 patients with different types of malignancies and the patient images reconstructed by TrueX algorithms.

No.	lesion max (KBq/ml)	bkg avg (KBq/ml)	Lesion dia(cm)	lesion: bkg ratio	RC	Pvcorr (kBq/mL)	SUV (g/ml) AFTER	SUV (g/ml) BEFOR	AFTER/BEFOR
1	33.48	5.0	2.4	6.7	0.68462	46.6	8.63	6.2	1.39
2	40.17	7.9	2.2	5.1	0.68484	55.0	7.06	5.15	1.37
3	32.448	2.9	1.8	11.2	0.68387	46.1	5.91	4.16	1.42
4	75.264	4.0	2	18.7	0.68271	108.4	22.58	15.68	1.44
5	99.12	2.3	1.7	43.0	0.67895	144.9	30.19	20.65	1.46
6	48.3	3.5	3	13.9	0.68342	69.1	11.51	8.05	1.43
7	45.18	4.6	2.7	9.9	0.68404	63.9	10.66	7.53	1.42
8	49.837	3.5	1.8	14.1	0.68340	71.3	16.58	11.59	1.43
9	35.088	3.7	1.8	9.6	0.68416	49.6	11.53	8.16	1.41
10	72.67	4.6	3.1	15.6	0.68318	104.2	24.24	16.9	1.43
11	28.733	3.2	1.8	9.0	0.68424	40.5	6.87	4.87	1.41
12	57.525	3.5	1.9	16.3	0.683085	82.6	14.00	9.75	1.44
13	29.9	5.3	2.4	5.6	0.68462	41.2	7.93	5.75	1.38
14	24.336	4.1	2.2	5.9	0.68468	33.7	6.47	4.68	1.38
15	35.508	5.9	2.2	6.0	0.68471	49.1	7.44	5.38	1.38
16	62.04	5.9	2.6	10.4	0.68399	88.0	13.33	9.4	1.42
17	47.428	5.0	1.8	9.5	0.68401	67.0	9.44	6.68	1.41
18	49.984	4.2	1.7	11.9	0.68375	71.2	10.02	7.04	1.42
19	54.315	5.0	1.8	10.8	0.68390	77.1	10.86	7.65	1.42

Table 6b: Parameters used for calculation of a partial volume corrected SUV_{max} for 19 lesions from 10 patients with different types of malignancies and the patient images reconstructed by OSEM algorithms.

No.	lesion max (KBq/ml)	bkg avg (KBq/ml)	Lesion dia(cm)	lesion: bkg ratio	RC	Pvcorr (kBq/ mL)	SUV (g/ml) AFTER	SUV (g/ml) BEFOR	AFTER/BEFOR
1	15.318	2.738	1.6	5.594595	0.6846	21.11155	2.85	2.07	1.38
2	12.284	4.218	1.5	2.912280	0.5882	17.93102	2.42	1.61	1.46

Table 7: represents the SUV values before and after applying RC model for NSCLC.

that ^{18}F-FDG uptake may be good prognostic of NSCLC outcome only through size dependence (i.e., larger non PVE-corrected tumors had higher ^{18}F-FDG recovery). This hypothesis is consistent with the observation that for tumors larger than 2.8 cm, which are thus weakly or not at all affected by PVE, there was no association between tumor stage and ^{18}F-FDG uptake.

Finally, this method could facilitate generation of equipment specific recovery coefficients for partial volume correction. The clinical implications for the increased accuracy in SUV determination are certainly of potential value in oncologic imaging (Table 7).

Competing Interests

The authors declare that they have no competing interests.

Acknowledgments

Great deepest thanks for excellent help and encouragement to Ass. Prof. Dr Sameh Reda chairman of Photometry department at NIS and Prof. Dr. Walid Omar chairman of nuclear medicine department at CCH.

Authors would also like to thank Nuclear Medicine Department team at CCH, for their assistance and support in accomplishing this work and also thank Femto Trade Company for their kind discount of hollow spheres phantom sets.

References

1. Ferretti A, Bellan E, Gava M, Chondrogiannis S, Massaro A, et al. (2012) Phantom study of the impact of reconstruction parameters on the detection of mini- and micro-volume lesions with a low-dose PET/CT acquisition protocol. Eur J Radiol 81: 3363-3370.
2. Shankar LK, Hoffman JM, Bacharach S, Graham MM, Karp J, et al. [2006] Consensus Recommendations for the Use of 18F-FDG PET as an Indicator of Therapeutic Response in Patients in National Cancer Institute Trials. J Nucl Med June 47: 1059-1066.
3. Adams MC, Turkington TG, Wilson JM, Wong TZ (2010) "A Systematic Review of the Factors Affecting Accuracy of SUV Measurements". American Journal of Roentgenology 195: 310-320.
4. Soret M, Bacharach SL, Buvat I (2007) Partial-volume effect in PET tumor imaging. J Nucl Med 48: 932-945.
5. Knäusl B, Hirtl A, Dobrozemsky G, Bergmann H, Kletter K, et al. (2012) PET based volume segmentation with emphasis on the iterative TrueX algorithm. Z Med Phys 22: 29-39.
6. Schöder H, Erdi YE, Chao K, Gonen M, Larson SM, et al. (2004) Clinical Implications of Different Image Reconstruction Parameters for Interpretation of Whole-Body PET Studies in Cancer Patients. J Nucl Med 45: 559-566.
7. Kapoor V, McCook BM, Torok FS (2004) An introduction to PET-CT imaging. Radiographics 24: 523-543.
8. http://www.nema.org/Standards/ComplimentaryDocuments/Contents%20and%20Scope%20NEMA%20NU%202%202012.pdf.
9. Srinivas SM, Dhurairaj T, Basu S, Bural G, Surti S, et al. (2009) A recovery coefficient method for partial volume correction of PET images. Ann Nucl Med 23: 341-348.
10. Perrine T, Stute S, Grotus N, Doyeux K, Hapdey S, et al. (2010) Comparative Assessment of Methods for Estimating Tumor Volume and Standardized Uptake Value in 18F-FDG PET. J Nucl Med 51: 268-276.
11. Daisne JF, Sibomana M, Bol A, Doumont T, Lonneux M, et al. (2003) Tri-dimensional automatic segmentation of PET volumes based on measured source-to-background ratios: influence of reconstruction algorithms. Radiother Oncol 69: 247-250.
12. Mohymen A, Mostafa S, Sultan A, Farag H (2014) "Phantom Study of the Impact of Activity Concentration (Tumor Uptake) On the Detection of Different Volume Lesions". Isotope and Radiation Research 46: 163: 175.
13. Jentzen W, Freudenberg L, Eising EG, Heinze M, Brandau W, et al. (2007) Segmentation of PET volumes by iterative image thresholding. J Nucl Med 48: 108-114.
14. Gupta A, Sharma P, Patel CD, Maharjan S, Pandey A, et al. (2011) Size-dependent thresholding as an optimal method for tumor volume delineation on positron emission tomography-computed tomography: A Phantom study. Indian J Nucl Med 26: 22-26.
15. Cheebsumon P, Yaqub M, van Velden FHP, Hoekstra OS, Lammertsma AA, et al. (2011) Impact of [18F]FDG PET imaging parameters on automatic tumor delineation: need for improved tumor delineation methodology Eur J Nucl Med Mol Imaging. 38: 2136-2144.
16. Rosslyn (2001) "National Electrical Manufacturers Association. NEMA Standards Publication NU 2-2001: Performance Measurements of Positron Emission Tomographs. National Electrical Manufacturers Association; dea. unsj.edu.ar/mednuclear/PET- NEMA-NU2-2001. p. 47.
17. Herzog H, Hichwa RD (2000) "Image reconstruction, quantification and standard uptake value". PET in Clinical Oncology book, link.springer.com, pp. 17-32.